Electrocatalysis

DOI: 10.1002/ange.201303495

Nickel/Nickel(II) Oxide Nanoparticles Anchored onto Cobalt(IV) Diselenide Nanobelts for the Electrochemical Production of Hydrogen**

*Yun-Fei Xu, Min-Rui Gao, Ya-Rong Zheng, Jun Jiang, and Shu-Hong Yu**

Dedicated to Professor Xiao-Zeng You on the occasion of his 80th birthday

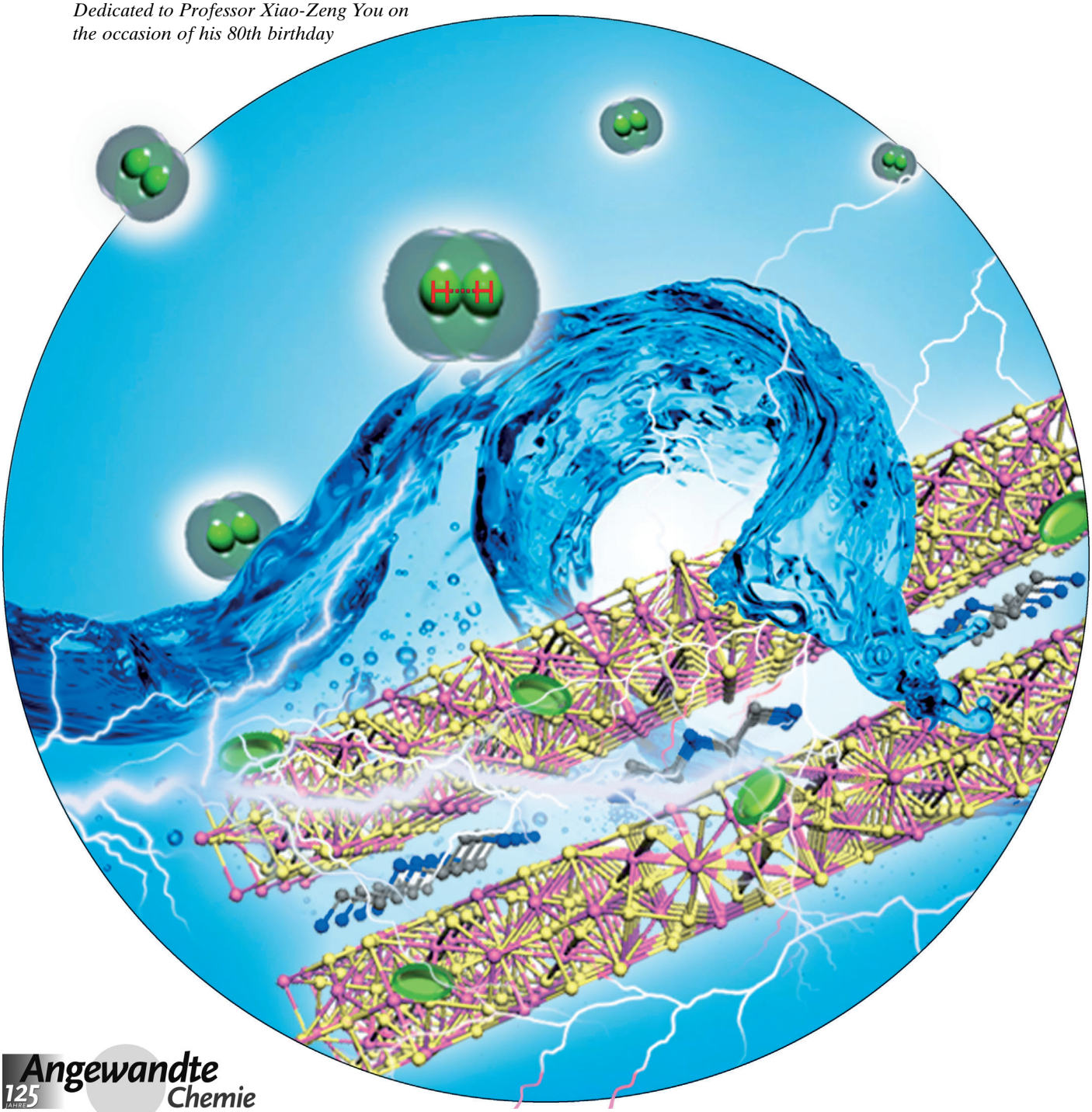

Hydrogen is one of the cleanest and most efficient energy carriers in our life. In particular, sustainable hydrogen production from water splitting has become an important issue.[1] To date, efficient electrocatalysts for the hydrogen evolution reaction (HER) are still expensive platinum-group metals. Searching for alternative Pt-free catalysts for the HER is a crucial task for hydrogen-based energy industry.

H_2 production is naturally catalyzed by the enzymes containing iron and nickel (Ni) ions.[1b,c,d] Inspired by the abundant element Ni (90 ppm) used in nature[1b,c] and detailed theoretical analyses,[2] various Ni-based materials have been designed to catalyze the HER, including, for example, Li^+-$Ni(OH)_2$-Pt,[2b] nickel diphosphine complex,[3] Raney Ni-Sn,[4] Ni-Al,[5] Ni-Mo alloys,[6] Raney Ni-Co_3O_4 matrix composite,[7] Ni dendrites,[8] and NiSe nanofiber assemblies.[9] However, these catalysts always faced the problems of low yield, synthetic difficulties, and especially the unsatisfactory catalytic properties. It is highly necessary to develop a simple strategy toward the fabrication of an economical and efficient Ni-based material for electrocatalytic hydrogen production.

Non-noble metal chalcogenides, typically MoS_2, have been intensively investigated as promising alternative catalysts for the HER.[10] The active edge sites on the MoS_2 nanoparticles (NPs) are verified to be effective for the HER.[10e] In our recent studies, novel lamellar mesostructured $CoSe_2$/DETA (DETA = diethylenetriamine) nanobelts (NBs) synthesized by a solvothermal strategy[11] were found to be very active for the oxygen evolution reaction (OER)[12] and oxygen reduction reaction (ORR),[13] and these electrocatalytic properties can be further enhanced by synergistic coupling with other functional nanostructures.[12,13] All above-mentioned research suggests that Ni species functionalized $CoSe_2$ NBs could be a promising catalyst for the HER.

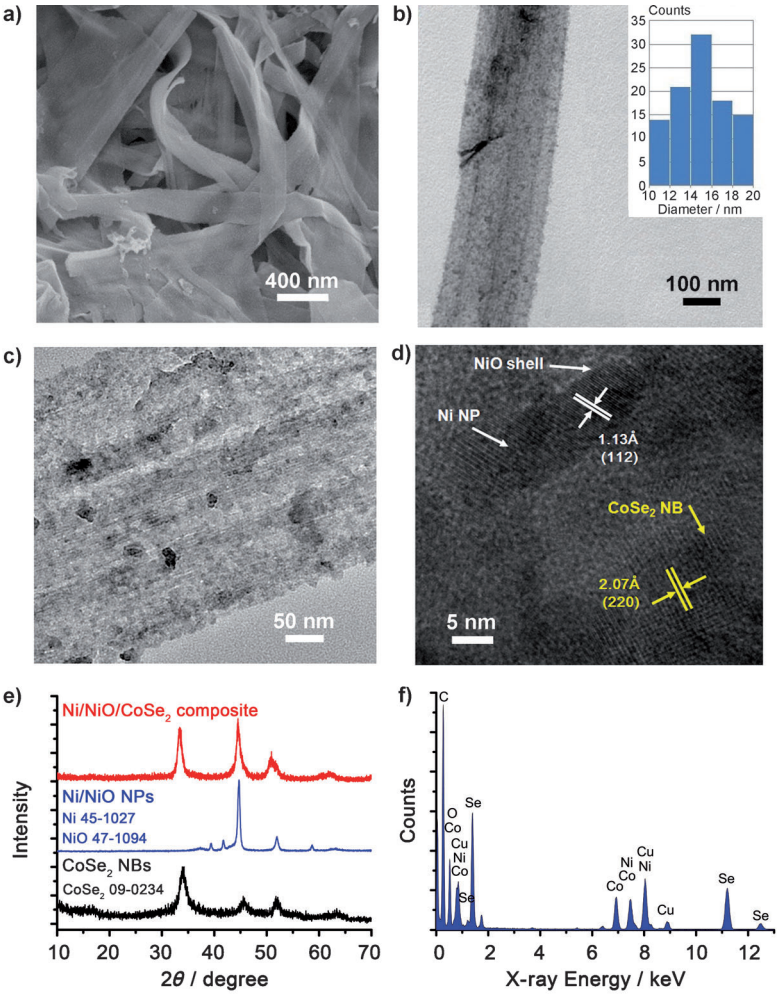

Figure 1. a) SEM image of the Ni/NiO/$CoSe_2$ nanocomposite. b,c) TEM images with different magnifications of the Ni/NiO/$CoSe_2$ nanocomposite. The inset in (b) shows the corresponding particle-size histogram. d) HRTEM image of an attached NP and its connected support. e) XRD patterns and f) EDX spectrum of the nanocomposite.

Herein, we report a simple solvothermal method to prepare Ni/$CoSe_2$ nanocomposite and a subsequent annealing process to form thin NiO shells on Ni NPs. This resulting novel Ni/NiO/$CoSe_2$ hybrid shows an excellent activity for the HER in acidic medium.

The Ni/$CoSe_2$ nanocomposite is synthesized by a simple solvothermal reaction in the solution of *N*,*N*-dimethylformamide (DMF). Then the thin NiO shells are formed by a thermal annealing process (see the Experimental Section). Figure 1 a–c shows the scanning electron microscopy (SEM) and transmission electron microscopy (TEM) images of the Ni/NiO/$CoSe_2$ nanocomposite with different magnifications. Figure 1 a and b shows that the substrate material of $CoSe_2$ NBs is thin, flexible, smooth, and almost transparent. The NBs have a width of 100–500 nm and lengths up to several tens of micrometers. Figure 1 b and c shows that the surfaces of the NBs are decorated by small NPs with an average diameter of about 15 nm (Figure 1 b and inset). The high-

[*] Y. F. Xu,[+] Dr. M. R. Gao,[+] Y. R. Zheng, Dr. J. Jiang, Prof. Dr. S. H. Yu
Division of Nanomaterials & Chemistry
Hefei National Laboratory for Physical Sciences at Microscale
Department of Chemistry, University of Science and Technology of China
Hefei 230026 (P. R. China)
E-mail: shyu@ustc.edu.cn
Homepage: http://staff.ustc.edu.cn/~yulab
[+] These authors contributed equally to this work.

[**] S. H. Yu acknowledges the funding support from the National Basic Research Program of China (grant number 2010CB934700), the National Natural Science Foundation of China (grant numbers 91022032, 91227103, and 21061160492), the Ministry of Science and Technology of China (grant number 2012BAD32B05-4), the Chinese Academy of Sciences (grant number KJZD-EW-M01-1), and the Principal Investigator Award by the National Synchrotron Radiation Laboratory at the University of Science and Technology of China.

Supporting information for this article is available on the WWW under http://dx.doi.org/10.1002/anie.201303495.

resolution TEM (HRTEM) image (Figure 1 d) shows a specific NP on the $CoSe_2$ NB, which uncovers the resolved lattice fringes of Ni (112) planes with a spacing of 1.13 Å, as well as (220) planes of the neighboring $CoSe_2$ substrate with a spacing of 2.07 Å. The X-ray diffraction (XRD) technique confirms the phases for the Ni/NiO/$CoSe_2$ nanocomposite, which corresponds to Ni (JCPDS 45-1027), NiO (JCPDS 47-1049), and $CoSe_2$ (JCPDS 9-234) (Figure 1 e). The NiO peaks are not obvious in that the NiO shells are too thin to emanate distinguishable peaks. Energy-dispersive X-ray spectroscopy (EDX) analysis confirms the existence of Ni, O, Co, and Se elements whereas Cu and C peaks emanating from the carbon-coated TEM grid also exist (Figure 1 f). The X-ray photoelectron spectroscopy (XPS) shows the surface electron states of the elements (see Figure S2 in the Supporting Information). The binding energies of Ni 2p and O 1s are 855.4 and 531.1 eV, respectively, which agree with the reported values of NiO (Ni 2p 855.6 eV, O 1s 531.2 eV).[14]

Anchoring Ni/NiO NPs onto the $CoSe_2$/DETA surface is easily achieved through a heterogeneous nucleation process, as illustrated in Figure 2. The confined growth of Ni on the $CoSe_2$/DETA surface is attributed to the copious amino groups on the $CoSe_2$/DETA surface (see Figure S3 in the Supporting Information), which can serve as the nucleation sites to couple Ni precursors and lead to corresponding deposition of Ni NPs on $CoSe_2$ under solvothermal condition.[12,13] The FT-IR spectrum shows that no DETA molecules remain on the obtained Ni/NiO/$CoSe_2$ nanocomposite (see Figure S3 in the Supporting Information), which should be the result of both Ni/NiO NP coverage and the high-temperature and pressure reaction. The same synthesis strategy produced free Ni/NiO core/shell NPs with a diameter of about 100 nm in the absence of $CoSe_2$ (Figure 2 c and d). Such obvious morphology difference demonstrates the mediating role of the $CoSe_2$ NBs, which could control the growth behavior of the introduced functional nanomaterials.

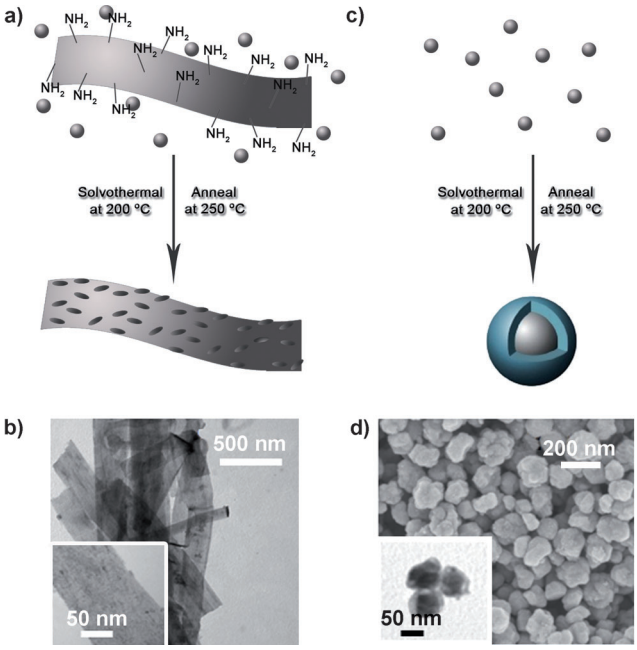

Figure 2. a) Synthesis of the Ni/NiO/$CoSe_2$ nanocomposite. b) TEM and HRTEM (inset) images of the Ni/NiO/$CoSe_2$ nanocomposite. c) Synthesis without any $CoSe_2$ NBs, resulting in large, free Ni/NiO core/shell NPs. d) SEM and TEM (inset) images of the free Ni/NiO core/shell NPs.

We investigated the catalytic performance for the HER of the Ni/NiO/$CoSe_2$ nanocomposite deposited on a glassy carbon (GC) electrode in Ar-saturated 0.5 M H_2SO_4 solution using a typical three-electrode setup (see the Supporting Information for measurement details). The $CoSe_2$ NBs, free Ni/NiO NPs, commercial Pt/C catalyst (Johnson–Matthey, 20 wt %), and bare glassy carbon (GC) electrode were also performed with the same measurement for comparison. Potentials are reported versus the reversible hydrogen electrode (RHE, see the Supporting Information for the calibration of the RHE). The polarization curves recorded on the Ni/NiO/$CoSe_2$ and $CoSe_2$ catalysts show onset potentials at about −0.03 and −0.05 V, respectively, beyond which the cathodic currents rise rapidly when the potential turns more negative, exhibiting superior activity than the well-studied Pt-free catalysts (Figure 3 a and Table S1).[3a,c,6,8,9,10b,c,d,e] In sharp contrast, the free Ni/NiO core/shell NPs catalyst has a small activity for the HER and the bare GC electrode does not affect the activity for the HER. The linear regions of the Tafel plots (Figure 3 b) were fit into the Tafel equation ($\eta = b\log(j) + a$, where b is the Tafel slope), yielding values of about 39, 48, and 30 mV per decade for the Ni/NiO/$CoSe_2$ nanocomposite, $CoSe_2$ NBs, and the commercial Pt/C catalyst, respectively. Compared with the Tafel slopes of other Pt-free catalysts like NiSe nanofiber assemblies[9] (about 64 mV per decade), core/shell MoO_3/MoS_2 nanowires[10b] (about 50–60 mV per decade), amorphous MoS_2 catalyst[10c] (about 60 mV per decade), and MoS_2/graphene[10d] catalyst (about 41 mV per decade), the lower Tafel slopes of our Ni/NiO/$CoSe_2$ nanocomposite and $CoSe_2$ NBs demonstrate their superior activities. To further assess the intrinsic activity of the new composite catalyst, the exchange current density (j_0) was also measured. The j_0 for the Ni/NiO/$CoSe_2$ nanocomposite was determined as 1.4×10^{-2} mA cm^{-2}, outperforming the value of 8.4×10^{-3} mA cm^{-2} of pure $CoSe_2$. Although the j_0 for the Ni/NiO/$CoSe_2$ nanocomposite is still much lower than that of the commercial Pt/C catalyst of 7.2×10^{-1} mA cm^{-2}, it is a satisfactory value for a Pt-free catalyst for the HER at the current state of the art.

The annealing temperature could significantly influence the activities for the HER of the Ni/NiO/$CoSe_2$ catalysts. The sample annealed at 250 °C for 1 h displays the best activity for the HER compared with its counterparts (Figure 3 c). The annealing process could remarkably improve the activity for the HER of the nanocomposite by forming synergistic NiO shells whereas the over-oxidized NiO shells will increase the internal resistance and block the active sites on the $CoSe_2$ nanobelts as a result of the high-temperature annealing. The sample annealed at 250 °C for 1 h produces the most compact and balanced core/shell configuration to take full advantage of the synergistic coupling effect from the functional materials.

Electrochemical impedance spectroscopy (EIS) measurements were performed for Ni/NiO/$CoSe_2$ nanocomposite and

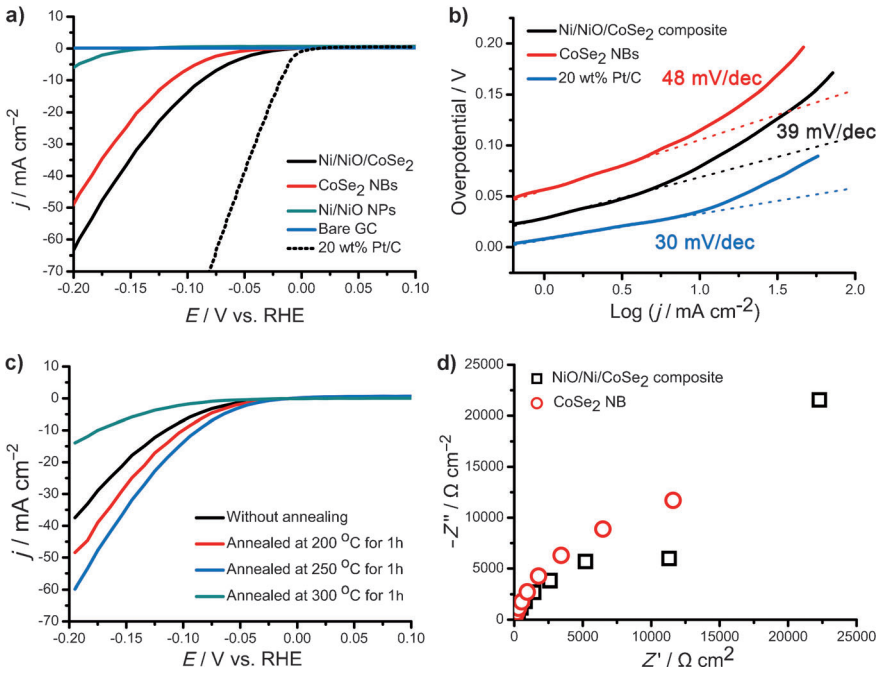

Figure 3. a) Polarization curves for the HER on a bare glassy carbon (GC) electrode and modified GC electrodes comprising the Ni/NiO/$CoSe_2$ nanocomposite, $CoSe_2$ NBs, Ni/NiO NPs, and a commercial 20 wt% Pt/C catalyst, respectively. b) Tafel plots derived from (a). c) Polarization curves for the HER on modified GC electrodes comprising Ni/NiO/$CoSe_2$ nanocomposites with different annealing treatments. d) Nyquist plots of the Ni/NiO/$CoSe_2$ nanocomposite and $CoSe_2$ NBs. Z' is the real impedance and $-Z''$ is the imaginary impedance. Catalyst loading: about 0.28 mg cm^{-2}. Sweep rate: 2 mV s^{-1}.

$CoSe_2$ NB samples to understand the enhanced electrochemical activation behavior (Figure 3d). The observed semicircle for the two samples suggests that the charge-transfer resistance controls the kinetics at the electrode interface.[18] The Ni/NiO/$CoSe_2$ nanocomposite exhibits a much smaller charge-transfer resistance, which is beneficial to achieve highly efficient charge transport, owing to the synergistic improvement from the loaded Ni/NiO nanoparticles. The Ni/NiO/$CoSe_2$ catalyst does not guarantee the long-term durability presumably because of the irreversible reaction of loaded Ni species in acidic medium. The unstable but efficient MoS_2 catalysts[10a,c] for the HER could be remarkably stabilized by anchoring graphene molecules onto their surface.[10d,f,g] The stability of the Ni/NiO/$CoSe_2$ catalyst could be much improved by incorporation of other protective materials, such as conductive graphene molecules, which is our ongoing work.

The experimentally observed excellent activity for the HER of our Ni/NiO/$CoSe_2$ nanocomposite catalyst agrees well with the reported theoretical analyses.[2] According to Greeley et al.,[2d] Ni is the most active metal among the non-noble metals for catalyzing the HER based on calculations derived from density functional theory (DFT) and the sabatier principle.[2a,d] On the other hand, Thiel et al.[2c] proposed that 3d transition-metal oxides (e.g. nickel oxide) are particularly active for catalyzing the HER, for that they are rich in defects for the dissociative adsorption of water molecules.[2b,c] Subbaraman et al.[2b] proposed that the edges of the nanometer-scaled Ni-(hydr)oxide clusters could facilitate the dissociation of water by weakening the O–H bond of the absorbed water. This assumption is experimentally verified by the $Ni(OH)_2$ cluster-modified Pt electrode surface.[2b] For our material, probably the Ni cores are also active for catalyzing the HER except for their function as conductive pathways, whereas NiO shells have the same promoting role to weaken the O–H bond in the absorbed water molecules.

The compact and balanced configuration of the core/shell structure on the smooth substrate of our catalyst plays a key role in enhancing the activity for the HER (Figure 4a). The modified $CoSe_2$ NB substrate could provide rich active sites for the HER reaction, the conductive Ni cores could efficiently lower the internal resistance, and the thin NiO shells could synergistically facilitate the dissociation of water. The conductive network of the Ni cores could also guarantee its commercial production at a large scale. Besides, the high density of the grain boundaries as a result of the very small particle size of the NiO shells creates efficient diffusion pathways for the H^+ ions.[16]

The chemical synergistic effect between the $CoSe_2$ NB substrate and the NiO shells also contributes to the enhanced activity. Notably, the free $CoSe_2$ NBs have a relatively high

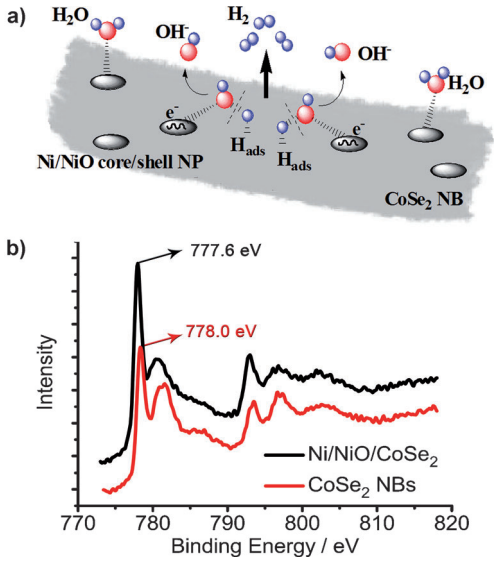

Figure 4. a) Dissociation of water, formation of H_{ads} intermediates, and subsequent recombination of two H_{ads} atoms to form H_2 as well as desorption of OH^- ions from the Ni/NiO core/shell domains. b) Co 2p XPS spectra for the free $CoSe_2$/DETA NBs and the as-constructed Ni/NiO/$CoSe_2$ nanocomposite.

activity for catalyzing the HER (Figure 3a–c), showing its role as a functional catalyst for water splitting.[15] On the other hand, the NiO shell functions as a synergist. Figure 4b shows that the electron-binding energy of Co 2p in $CoSe_2$ decreases by 0.4 eV after being decorated by Ni/NiO core/shell NPs (Figure 4b). This is presumably caused by the electron transfer from the NiO shells to the $CoSe_2$ substrate.[12] Then the more Lewis acidic NiO shells further facilitate the activation of Lewis basic H_2O through Lewis acid–base interaction, which finally leads to an improved activity for the HER. Thus, this work represents a new strategy for constructing advanced electrocatalysts for the HER with high performance by coupling different multifunctional materials together.

Generally, there are three principal steps that could participate for the HER in acidic media,[9,10b,d,17] that is, the Volmer (electrochemical hydrogen adsorption: $H_3O^+ + e^- \rightarrow H_{ads} + H_2O$), the Heyrovsky (electrochemical desorption: $H_{ads} + H_3O^+ + e^- \rightarrow H_2\uparrow + H_2O$), and the Tafel (chemical desorption: $H_{ads} + H_{ads} \rightarrow H_2\uparrow$) reactions. According to the kinetic models for the HER, Tafel slopes of about 120, 40, or 30 mV per decade will be achieved if the Volmer, Heyrovsky, or Tafel step is the rate-determining step, respectively.[17] The experimentally observed Tafel slope of about 39 mV per decade for the Ni/NiO/$CoSe_2$ catalyst suggests that the Volmer–Heyrovsky mechanism takes effect in the HER.[17]

In summary, we report a cheap and advanced catalyst for the HER of the Ni/NiO/$CoSe_2$ nanocomposite, which can be synthesized by anchoring Ni/NiO nanoparticles onto $CoSe_2$ nanobelts through a simple solvothermal reaction and a subsquent thermal annealing process. Such a composite catalyst shows a small cathodic onset potential of about −0.03 V and a small Tafel slope of about 39 mV per decade. To our knowledge, this new nanocomposite catalyst is one of the best Pt-free electrocatalysts for the HER in acidic medium. The enhanced property may be attributed to the compact configuration of the Ni/NiO core/shell NPs anchored onto the spacious $CoSe_2$ NBs. This work presents a new strategy for designing advanced non-noble metal catalysts by coupling multifunctional nanostructures together and can be extended for developing new composite catalysts in the future.

Received: April 25, 2013
Published online: July 10, 2013

Keywords: cobalt · electrocatalysis · electrochemistry · hydrogen evolution reaction · nickel

[1] a) K. Mazloomi, C. Gomes, *Renewable Sustainable Energy Rev.* **2012**, *16*, 3024–3033; b) B. E. Logan, S. E. Oh, I. S. Kim, S. V. Ginkel, *Environ. Sci. Technol.* **2002**, *36*, 2530–2535; c) J. Rossmeisl, K. Dimitrievski, P. Siegbahn, J. K. Norskov, *J. Phys. Chem. C* **2007**, *111*, 18821–18823; d) K. Maeda, K. Domen, *J. Phys. Chem. Lett.* **2010**, *1*, 2655–2661; e) L. Y. Zhang, C. X. Guo, Z. M. Cui, J. Guo, Z. L. Dong, C. M. Li, *Chem. Eur. J.* **2012**, *18*, 15693–15698; f) Y. Qiao, S. J. Bao, C. M. Li, *Energy Environ. Sci.* **2010**, *3*, 544–553; g) M. R. Gao, Y. F. Xu, J. Jiang, S. H. Yu, *Chem. Soc. Rev.* **2013**, *42*, 2986–3017.

[2] a) A. B. Laursen, A. S. Varela, F. Dionigi, H. Fanchiu, C. Miller, O. L. Trinhammer, J. Rossmeisl, S. Dahl, *J. Chem. Educ.* **2012**, *89*, 1595–1599; b) R. Subbaraman, D. Tripkovic, D. Strmcnik, K. C. Chang, M. Uchimura, A. P. Paulikas, V. Stamenkovic, N. M. Markovic, *Science* **2011**, *334*, 1256–1260; c) P. A. Thiel, *Surf. Sci. Rep.* **1987**, *7*, 211–385; d) J. Greeley, T. F. Jaramillo, J. Bonde, I. Chorkendorff, J. K. Norskov, *Nat. Mater.* **2006**, *5*, 909–913.

[3] a) J. Y. Yang, S. T. Chen, W. G. Gougherty, W. S. Kassel, R. M. Bullock, D. L. DuBois, S. Raugei, M. Dupuis, M. R. DuBois, *Chem. Commun.* **2010**, *46*, 8618–8620; b) A. Le Goff, V. Artero, B. Jousselme, P. D. Tran, N. Guillet, R. Metaye, A. Fihri, S. Palacin, M. Fontecave, *Science* **2009**, *326*, 1384–1387; c) U. J. Kilgore, J. A. S. Roberts, D. H. Pool, A. M. Appel, M. P. Stewart, M. R. DuBois, W. G. Dougherty, W. S. Kaeel, R. M. Bullock, D. L. DuBois, *J. Am. Chem. Soc.* **2011**, *133*, 5861–5872; d) J. Y. Yang, R. M. Bullock, W. J. Shaw, B. Twamley, K. Fraze, M. R. DuBois, D. L. DuBois, *J. Am. Chem. Soc.* **2009**, *131*, 5935–5945.

[4] G. W. Huber, J. W. Shabaker, J. A. Dumesic, *Science* **2003**, *300*, 2075–2077.

[5] J. Dulle, S. Nemeth, E. V. Skorb, T. Irrgang, J. Senker, R. Kempe, A. Fery, D. V. Andreeva, *Adv. Funct. Mater.* **2012**, *22*, 3128–3135.

[6] N. V. Krstajic, V. D. Jovic, L. G. Krstajic, B. M. Jovic, A. L. Antozzi, G. N. Martelli, *Int. J. Hydrogen Energy* **2008**, *33*, 3676–3687.

[7] G. Schiller, R. Henne, P. Mohr, V. Peinecke, *Int. J. Hydrogen Energy* **1998**, *23*, 761–765.

[8] S. H. Ahn, S. J. Hwang, S. J. Yoo, I. Choi, H. J. Kim, J. H. Jang, S. W. Nam, T. H. Lim, T. Lim, S. K. Kim, J. J. Kim, *J. Mater. Chem.* **2012**, *22*, 15153–15159.

[9] M. R. Gao, Z. Y. Lin, T. T. Zhuang, J. Jiang, Y. F. Xu, Y. R. Zheng, S. H. Yu, *J. Mater. Chem.* **2012**, *22*, 13662–13668.

[10] a) B. Hinnemann, P. G. Moses, J. Bonde, K. P. Jorgensen, J. H. Nielsen, S. Horch, I. Chorkendorff, J. K. Norskov, *J. Am. Chem. Soc.* **2005**, *127*, 5308–5309; b) Z. B. Chen, D. Cummins, B. N. Reinecke, E. Clark, M. K. Sunkara, T. F. Jaramillo, *Nano Lett.* **2011**, *11*, 4168–4175; c) J. D. Benck, Z. B. Chen, L. Y. Kuritzky, A. J. Forman, T. F. Jaramillo, *ACS Catal.* **2012**, *2*, 1916–1923; d) Y. G. Li, H. L. Wang, L. M. Xie, Y. Y. Liang, G. S. Hong, H. J. Dai, *J. Am. Chem. Soc.* **2011**, *133*, 7296–7299; e) T. F. Jaramillo, K. P. Jorgensen, J. Bonde, J. H. Nielsen, S. Horch, I. Chorkendorff, *Science* **2007**, *317*, 100–102; f) H. L. Wang, H. J. Dai, *Chem. Soc. Rev.* **2013**, *42*, 3088–3113; g) Y. Y. Liang, Y. G. Li, H. L. Wang, H. J. Dai, *J. Am. Chem. Soc.* **2013**, *135*, 2013–2036.

[11] M. R. Gao, W. T. Yao, H. B. Yao, S. H. Yu, *J. Am. Chem. Soc.* **2009**, *131*, 7486–7487.

[12] M. R. Gao, Y. F. Xu, J. Jiang, Y. R. Zheng, S. H. Yu, *J. Am. Chem. Soc.* **2012**, *134*, 2930–2933.

[13] a) M. R. Gao, Q. Gao, J. Jiang, C. H. Cui, W. T. Yao, S. H. Yu, *Angew. Chem.* **2011**, *123*, 5007–5010; *Angew. Chem. Int. Ed.* **2011**, *50*, 4905–4908; b) M. R. Gao, S. Liu, J. Jiang, C. H. Cui, W. T. Yao, S. H. Yu, *J. Mater. Chem.* **2010**, *20*, 9355–9361.

[14] S. Uhlenbrock, C. Scharfschwerdt, M. Neumann, G. Illing, H. J. Freund, *J. Phys. Condens. Matter* **1992**, *4*, 7973–7978.

[15] V. Artero, M. Chavarot-Kerlidou, M. Fontecave, *Angew. Chem.* **2011**, *123*, 7376–7405; *Angew. Chem. Int. Ed.* **2011**, *50*, 7238–7266.

[16] Q. Lu, M. W. Lattanzi, Y. P. Chen, X. M. Kou, W. F. Li, X. Fan, K. M. Unruh, J. G. Chen, J. Q. Xiao, *Angew. Chem.* **2011**, *123*, 6979–6982; *Angew. Chem. Int. Ed.* **2011**, *50*, 6847–6850.

[17] B. E. Conway, B. V. Tilak, *Electrochim. Acta* **2002**, *47*, 3571–3594.

[18] a) W. F. Chen, C. H. Wang, K. Sasaki, N. Marinkovic, W. Xu, J. T. Muckerman, Y. Zhu, R. R. Adzic, *Energy Environ. Sci.* **2013**, *6*, 943–951; b) B. Losiewicz, A. Budniok, E. Rowinski, E. Lagiewka, A. Lasia, *Int. J. Hydrogen Energy* **2004**, *29*, 145–157.

